Energy, Mines and Resources Canada | Énergie, Mines et Ressources Canada

CANMET

Canada Centre for Mineral and Energy Technology | Centre canadien de la technologie des minéraux et de l'énergie

DISBONDING OF STAINLESS STEEL WELD OVERLAY FOLLOWING SIMULATED PRESSURE VESSEL SERVICE EXPOSURE

M. GODDEN and L. SETO
METALLURGY SECTION

OCTOBER, 1983

This document is an unedited internal report prepared primarily for discussion and information purposes. It does not represent a final expression of the opinion of the Canada Centre for Mineral and Energy Technology (CANMET)

Ce document est un rapport préliminaire non-révisé et rédigé principalement pour fin de discussion et de documentation interne. Il ne représente nullement l'expression définitive de l'opinion du Centre canadien de la technologie des minéraux et de l'énergie (CANMET)

ENERGY RESEARCH PROGRAM

MICROMEDIA
JUL 2 8 1984

31pp

PHYSICAL METALLURGY RESEARCH LABORATORIES
REPORT: ERP/PMRL 83-69(TR)

PHYSICAL METALLURGY RESEARCH LABORATORIES
REPORT ERP/PMRL 83-69(TR)

DISBONDING OF STAINLESS STEEL WELD OVERLAY FOLLOWING SIMULATED PRESSURE VESSEL SERVICE EXPOSURE

by

M. Godden and L. Seto

ABSTRACT

Hydrogen in solution in the walls of pressure vessels having an overlayed stainless steel inner surface can cause disbonding after service. The microstructural features associated with this phenomenon have been examined on two specimens after exposure to simulated pressure vessel conditions of 454°C for 46 h in 17.2 MPa hydrogen in an autoclave. A computer program to describe hydrogen profiles through the walls during pressure vessel operation and shutdown is also given. The important factors influencing disbonding are discussed in terms of pressure vessel manufacture and operation, and suggestions for future work outlined.

LABORATOIRES DE RECHERCHE EN MÉTALLURGIE PHYSIQUE
RAPPORT PRE/LRMP 83-69(TR)

CONTRÔLE DE LA FISSURATION DES SOUDURES DES PAROIS EN ACIER INOXYDABLE DES RÉCIPIENTS SOUS PRESSION PAR UNE OPÉRATION EN SERVICE SIMULÉE

par

M. Godden et L. Seto

RÉSUMÉ

L'hydrogène en solution dans les parois en acier inoxydable des récipients sous pression peut causer la fissuration des soudures après usage. On a fait l'étude des particularités liées à ce phénomène en observant en autoclave deux échantillons soumis aux conditions thermiques simulées d'un récipient sous pression, soit 454°C pendant 46 h, la pression atmosphérique de l'hydrogène étant à 17,2 MPa. Les réactions qui se sont produites à l'intérieur du récipient ont été observées en cours d'opération et à l'arrêt au moyen d'un programme informatique. L'étude des éléments importants qui peuvent causer la fissuration porte sur la mise au point et le fonctionnement des récipients sous pression. En outre, des suggestions quant à l'orientation des recherches futures sont présentées.

INTRODUCTION

Crude oil refining at high pressures and temperatures in hydrogen containing and corrosive environments is frequently carried out in composite pressure vessels. Typically, these vessels have a thick outer wall of ferritic steel, usually of 2 1/4 Cr-1 Mo, to withstand the pressure and temperature and an inner surface of a corrosion-resistant stainless steel. This type of pressure vessel is particularly important for heavy oil upgrading, an operation likely to become increasingly important in Canada as conventional reserves are depleted and unconventional sources such as tar sands are exploited.

Hydrogenation pressure vessels are manufactured to the ASME Boiler and Pressure Vessel Code, Section VIII, Division 2. This code details the manufacturing and the design requirements. Typically these vessels operate at 400-450°C, 10-20 MPa pressure with a process stream of 70-98% H_2, which also contains H_2S, CH_4 and Cl^-. Polythionic acid and $H_nS_xO_y$ can also form during a shutdown. Typical vessels are 20-25 m high, 3-5 m diam with a 150-250 mm wall thickness. Although there are other ways, the most usual method of fabricating a vessel is to make rings which are welded one on top of another to form a cylindrical shell. A stainless steel overlay is deposited inside by welding and internal and external attachments are finally added by welding. The ASME Boiler and Pressure Vessel Code specifies that welding plate of these thicknesses (generally greater than 50 mm) must be followed by a post-weld heat-treatment (PWHT) to relieve thermally induced stresses. Furthermore, it also specifies the analysis range of the weld overlay at a certain depth. This is a difficult requirement to meet if only one layer of stainless steel is deposited because it is diluted by the underlying base material. Frequently, two layers are deposited instead, first a "butter" layer of a stainless steel rich in alloying elements is applied, then a second layer of the desired composition is applied on top. The weld deposition of strip stainless steel by the submerged-arc process is considered to be a welding process for the purposes of the ASME code and PWHT requirements apply. Indeed, during fabrication, a given region of overlayed material might be subject to several PWHT's depending on the complexity of the region and associated internal attachments.

During continuous service, hydrogen diffuses through the overlay and the base metal until a steady-state hydrogen flux is established. When the vessel is taken out of service and the pressure and temperature reduced to ambient, hydrogen within the vessel walls migrates towards the wall surfaces. However, hydrogen diffusion in ferritic steels is approximately two orders of magnitude faster than in stainless steels. High cooling rates of the vessel can lead to very high hydrogen concentrations at the stainless steel/base metal interface and in the stainless steel immediately adjacent to the interface. Clearly, the extent to which hydrogen concentrates on cooling depends upon pre-existing hydrogen concentrations and on the cooling rate. The condition at the interface of the stainless steel and base metal is further aggravated by the mixed microstructures produced as the composition varies continuously from base metal to stainless steel and also by the difference in thermal expansion between the stainless steel and base metal which causes thermally-induced stresses. All of these factors combine to produce "disbonding" at or near the interface. Disbonding takes the form of tight cracks at and parallel to the interface or in the stainless steel overlay immediately adjacent to it. The hazard has been described and investigated only recently, but is always present when operating an overlayed pressure vessel because emergency shutdowns cannot be avoided (1-4). Indeed, recently, large cracks attributed to disbonding have been reported in a Canadian refinery pressure vessel (5) as well as elsewhere (3).

In the current work, the objective was to make a preliminary investigation of disbonding with particular emphasis on microstructural factors, because little or nothing could be done to change the relative diffusion rates in ferritic and austenitic steels or the difference in thermal expansion between the two steels. Various techniques have been applied to examine the interface region, including exposing two samples of overlayed material with different thicknesses of overlay to conditions in an autoclave likely to promote disbonding.

EXPERIMENTAL METHODS

Overlayed material was produced by the strip submerged arc process in the PMRL Welding Section. Two samples were produced by overlaying 2 1/4 Cr-1 Mo plate 38 mm thick firstly with 309 stainless steel then with either

347 or 316 L. The material compositions are given in Table 1 and further details of the overlay process used may be obtained in (6). Sections of the two samples were taken perpendicular to the weld interface and examined by various techniques in three conditions (i) as-welded, (ii) after 6 h PWHT at 690°C, representing the minimum PWHT required for a 152 mm thick pressure vessel under the ASME Pressure Vessel Code, (iii) after 30 h PWHT at 690°C, representing the maximum PWHT time likely any overlay region might experience as a result of several internal attachments being made each followed by a PWHT. In both cases (ii) and (iii) heating and cooling rates satisfied the ASME Pressure Vessel Code (56°C/h).

Satisfactorily etching the stainless steel and 2 1/4 Cr-1 Mo steel simultaneously presents problems because of the differences in chemical reactivity of the two steels and of the transition zone between them. Several different methods were attempted before it was decided a two-part technique was most effective, the stainless steel being etched electrolytically at 5 V in 2% chromic acid, then the 2 1/4 Cr-1 Mo being etched in 2% nital. However, the transition zone tends to be less etched than other regions, particularly in the as-welded condition, and a step occurs at the interface if approximately the same amount of material is not removed by both etchants.

Various electron optical examination techniques were used in an attempt to examine fine scale microstructure. Direct carbon extraction replicas cannot be made because of the different rates of attack of the overlay and base metal. Two-stage plastic extraction replicas were made by replicating the etched surface with bioden film, depositing carbon on this film then dissolving it with acetone. Conventional electropolishing to produce thin foils cannot be used in the interface region because of the different chemical reactivities of the steels, but ion beam thinning could be used. Two thin foils were made by ion beam thinning but the results were unsatisfactory with no thin areas and extensive surface oxidation. However, this technique still offers potential for thin foil preparation from the interface region. Etched samples were also examined in the Cambridge Instruments SEM 250.

Concentration profiles of Cr, Ni and Nb were made across the interface region in the as-welded and PWHT conditions. Knoop microhardness measurements were made of the same region using a 500 g load and a 10.25 mm objective.

Two samples PWHT 30 h at 690°C were prepared for simulated service exposure in an autoclave at the Energy Research Laboratories (ERL). Both samples were surface ground to 68 mm long by 49.5 mm wide and 31.5 mm thick with the overlay on the 68 mm x 49.5 mm surface. The sample of 309/347 overlay was ground to give an average overlay thickness of 5.0 mm whereas the sample of the 309/316 L overlay was ground to an overlay thickness of 7.0 mm. The 309/347 sample was drilled with a 1.19 mm diam flat-bottomed hole to the overlay depth near one corner as a reference hole for ultrasonic examination. The samples were exposed, one at a time, to hydrogen at 17.2 MPa pressure at 454°C for 46 h in an autoclave. At the completion of a run, the hydrogen pressure was released and the autoclave cooled by water in a cooling coil. This resulted in a cooling rate of 86.7°C/h. After 2 h cooling the specimens were removed from the autoclave.

The samples were ultrasonically inspected at intervals with a SFz 57A2215 transducer 8 mm diam operating at 5MHz following exposure to detect disbonding. Overnight, acoustic emission was used to detect cracking events.

A computer program was written to generate the theoretical profiles of the hydrogen concentrations in steady state service (or simulated service) conditions as well as during cooling. A complete description of the program including the equations and the diffusion coefficients used are given in Appendix I.

RESULTS

An example of the interface region of as-welded 309/347 overlay prepared for optical microscopy is shown in Fig. 1. The heat-affected-zone of the 2 1/4-1 Mo steel substrate is bainite, similar to the parent material but with a larger prior-austenite grain size. As the interface is approached, the 2 1/4 Cr-1 Mo steel etches lighter, blending into an almost unetched white band. Features in this band are discernible with difficulty, the structure being martensitic. There is a distinct interface between the martensite and the 309 overlay region. In the 309 overlay region immediately adjacent to the interface there is an absence of inclusions and δ-ferrite. However, further from the interface there are numerous spherical inclusions in the 309 stainless steel and the δ-ferrite outlines a clear dendritic pattern with the dendrites perpendicular to the interface. The example shown in Fig. 1 is not

typical of the interface region; generally the interface is approximately planar. However there are several regions, such as those shown in Fig. 1, where tongues or islands of 2 1/4 Cr-1 Mo steel (or modified 2 1/4 Cr-1 Mo steel) intrude into the 309 stainless layer. Figure 1 shows a long tongue of material at the interface and also an island further from the interface in the 309 stainless steel. The island shown is entirely austenitic, having no martensite interface of its own, although some larger islands have a ferritic core. Islands are tongues which are free of the interface in the plane of the specimen. It is not known if they are attached to the interface in some other plane.

The width of the martensitic band at the interface varies widely, being very wide, ~ 20 μm at intruding tongues, but much less, ~ 3 μm in the large planar interface regions. The intruding islands vary in size up to 0.7 mm long and 60 μm wide.

The most obvious change observable optically after post-weld heat-treatment (PWHT) is the tempering of the martensite band at the interface, which etches more darkly (Figs. 2 and 3). Another change observed is fine carbide precipitation in the tempered martensite and at the stainless steel grain boundaries adjacent to the interface. During prolonged PWHTs, the carbides grow. Scanning electron microscopy reveals the carbides much more clearly (Fig. 4). The largest carbides occur in the stainless steel grain boundaries and at the interface between martensite bands and the 2 1/4 Cr-1 Mo steel, those within the martensite being finer. Attempts at analysing these carbides in situ by energy dispersive X-ray methods were unsuccessful because of their small size and the similar chemistry of the background material. Two stage plastic replication was used to isolate carbides from the matrix, a technique which makes X-ray analysis and lattice parameter measurements easier by removing background effects. However, while the carbides were replicated, they were rarely extracted by this technique. An example of successful particle extraction is shown in Fig. 5. Energy dispersive X-ray analysis of this particle showed the presence of chromium and magnesium. Diffraction pattern data were insufficient to determine its space group symmetry or lattice parameters. Thus it was unknown if this was a carbide or chromium-rich magnesium slag inclusion resulting from the overlay process. Improvements in extraction efficiency will be needed before more conclusive carbide identification can be made by this technique.

The electron microprobe analyses adjacent to the interface of the 309/347 overlay in both the as-welded and PWHT conditions are shown in Fig. 6. Clearly, the concentration of the solute elements measured does not change significantly until very close to the interface and this situation is unaffected by the PWHT. However, the concentration of chromium and nickel increases at the interface after PWHT. Carbon measurements are not possible in the electron microprobe.

The microhardness results obtained across the interface before and after PWHT are shown in Fig. 7. The data points represent a mean of 5 measurements in the as-welded condition and 3 measurements after PWHT. Hardness measurements of the as-welded overlay showed considerable scatter, particularly for the 309/316 L overlay. The scatter was attributed to individual microstructural features. For example, the martensite band showed Knoop hardnesses up to 390. Reporting the results as a mean of 5 readings tends to obscure this scatter. There are some minor differences in hardness between the two overlays in the as-welded condition. This was probably caused by differences in welding conditions which resulted in differences in cooling rate and/or residual stresses. However, the PWHT eliminates these hardness differences. Based on these hardness results and microprobe analyses, it was concluded that the 309/316 L and 309/347 overlays are identical in the interface region after PWHT.

The two samples exposed to high pressure hydrogen in an autoclave were subsequently examined at intervals by ultrasonic methods and monitored for acoustic emission overnight. The 309/316 L sample with 7 mm overlay thickness showed one event of acoustic emission but no evidence of cracking was detected in any subsequent ultrasonic inspection. It was concluded that if any cracking did occur it was too small to be detected (i.e., significantly less than 1 mm diam). The 309/347 sample with 5 mm overlay thickness showed no cracking when ultrasonically inspected 3 h after the hydrogen pressure was released in the autoclave. However, there were many events detected by acoustic emmission overnight, 3 to 20 h after the hydrogen pressure was released in the autoclave. Subsequent ultrasonic inspection revealed four small crack sites at a depth corresponding to the interface. When the inspection was repeated several days later the four sites had amalgamated into one large crack site, as shown schematically in Fig. 8. A metallographic section close

to the perimeter of the detected crack site confirmed the ultrasonic inspection results, Fig. 9. However, there were also small cracks outside this area in the region that was ultrasonically sound. The crack was tight and almost continuous, mainly following the grain boundaries of the stainless overlay closest to the interface but also with excursions into the interface martensite. Very occasionally a small crack was observed in the 2 1/4 Cr-1 Mo HAZ and appeared to be associated with an elongated inclusion; in a mechanism analagous to stepwise cracking of controlled-rolled linepipe steels in sour environments.

The results of the computer simulation of the hydrogen profile at the completion of autoclave exposure and upon attaining ambient temperature (estimated 5 h after the hydrogen pressure was released in the autoclave) are illustrated in Fig. 10. These calculations are based solely on hydrogen ingress through the overlay surface. The hydrogen concentration in the stainless steel adjacent to the interface increased to 46 ppm, on cooling. The computer program is unable as yet to handle the development of hydrogen profiles after ambient temperature is reached and it is not known if the hydrogen concentration in this interface region continues to increase before ultimately declining.

DISCUSSION

Various metallographic techniques have been used to examine the interface region. The most effective etching technique was found to be one in which the stainless steel layer was first etched electrolytically at 5 V in 2% chromic acid and the 2 1/4 Cr-1 Mo steel etched in 2% nital, although care is necessary to ensure similar amounts of material are removed by both etches. Whereas this technique aids phase identification by appearance, specimen preparation techniques for analytical electron microscopy, such as electron diffraction and X-ray analysis, have been largely unsuccessful. Particle identification in the tempered martensite interface band and in the stainless steel grain boundaries adjacent to the interface after PWHT is particularly important because these are the preferential sites for subsequent disbonding cracks.

Optical examination revealed islands or intrusions of the 2 1/4 Cr-1 Mo steel into the overlay material. The mechanism for their occurrence

is unclear but is likely related to the dynamics of the weld pool rather than surface preparation prior to overlay welding. Similar features were observed in a sample of commercial overlay prepared by Japanese Steel (7). The intrusions in particular can have a significant effect on disbonding for two reasons. Firstly, the intrusions are sufficiently large that they interfere with the potential crack path, effectively acting to stop the crack, see Fig. 9. Secondly, even at small intrusions the martensite band width at the interface is increased. This results in more sites for carbon precipitation and less carbon availability for precipitation at stainless steel boundaries. Hence intrusions could be useful in reducing the severity of disbonding but their mechanism of formation and three-dimensional shape are unknown at present.

Comparison of the polished but unetched overlay samples of this work with those of a Japanese Steel overlay sample showed approximately twice as many spherical inclusions in the PMRL-produced overlays. However, the disbonding cracks were not observed associated with these inclusions and they are thought to play no part in the disbonding mechanism.

Blondeau et al (2) have described three essential conditions for disbonding to occur; (i) local high hydrogen concentration (ii) high stresses (iii) presence of a hydrogen embrittlement sensitive microstructure. In attempting to simulate the operation of a large pressure vessel, shortcomings in any of these conditions can occur experimentally. In the current work, (i) and (ii) are particularly different from commercial experience. The autoclave exposes all surfaces of the sample to the hydrogen atmosphere. Thus, hydrogen diffuses in to a higher concentration than that shown in the Fig. 10, particularly in the 2 1/4 Cr-1 Mo steel. Similarly, after autoclave exposure, hydrogen can diffuse out of the specimen from all surfaces. This probably accounts for the disbonding cracks being located at the interface furthest from any 2 1/4 Cr-1 Mo steel surface. High stresses are reported to result from the sum of welding-induced stresses incompletely removed by PWHT and stresses induced by differences in thermal expansion of the overlay and base metals. The small size of a sample in relation to a commercial pressure vessel limits the stresses which can be generated by these two mechanisms. The propagation of a disbonding crack requires a tensile stress component normal to the interface. Such a stress could result from differences in thermal contraction on cooling a pressure vessel but, because no restraint is applied to a sample, such stresses would be small. The essential condition (iii) was achieved

through the use of appropriate starting materials and PWHT. The PWHT chosen was representative of the sum of PWHT cycles following multiple welding and, therefore, represents the worst condition insofar as carbon (and other elements) diffusion is concerned. However, the 2 1/4 Cr-1 Mo steel plate had only 0.11% C, whereas the carbon content of thick-section 2 1/4 Cr-1 Mo steel plate, typical of a pressure vessel, is deliberately chosen to be at the high end of the specification range, i.e., ~ 0.14 to 0.15% C, to achieve sufficient hardenability (8). The rate of carbon diffusion into the overlay through the interface will depend on the carbon content difference between the overlay and base-metal, as demonstrated by Blondeau et al (2). Thus, although the carbon content at the interface of the sample was lower than might be expected from low carbon level of the base metal, it was enhanced by the long PWHT time.

Despite the above difficulties, disbonding was observed in the sample with 5 mm thick overlay and none (or very little) was observed in the 7 mm thick overlay sample. This brackets the conditions under which it can occur in the laboratory (assuming the 309/347 and 309/316 L behave identically with respect to disbonding). Further, it demonstrates the importance of overlay thickness. Under conditions of constant hydrogen flux (prolonged pressure vessel operation), the hydrogen concentration at the interface is lower for a thicker overlay, resulting in a lower hydrogen concentration spike upon cooling, as can be seen from an examination of Fig. 10. Clearly, from a pressure vessel design viewpoint the economics of thicker weld overlays must be weighed against the risk of disbonding.

The observed disbonding crack morphology agrees with the descriptions by other workers (2,9). Asami and Sahai (9) have described cracks in the overlay grain boundaries, martensitic band and in the base metal heat-affected-zone (HAZ). The cracks observed in this work occurred mainly in the overlay boundaries and the martensitic band with very little evidence of cracking in the base metal HAZ. The base metal HAZ cracks that were seen, appeared to have nucleated on large base metal inclusions, indicating a similar mechanism to hydrogen crack formation in stepwise cracking of HSLA steels. Nucleation of cracks at the inclusion/metal boundary does not occur in the stainless steel layer, despite much higher hydrogen levels near the interface, cracking being restricted to an alignment with carbides in the overlay grain boundaries. This could be related to the carbide surface boundary tension or the cracks initiating by trans-carbide fracture.

CONCLUSIONS

1. Various techniques have been used to examine the interface region of 309/347 and 309/316 L overlays. A two-stage etch; electrolytic 5 V in 2% chromic acid followed by 2% nital, was found to be most effective. Phase identification has been possible only on the basis of appearance. An improved two-stage plastic replica method could be useful for particle extraction and identification by X-ray or electron diffraction techniques.
2. Disbonding cracks were produced in a sample after autoclave exposure to 17.2 MPa pressure of hydrogen for 46 h at 454°C. The cracks required an incubation period to form and were located in the martensite band or adjacent overlay grain boundaries. They were typical of those reported by other workers.
3. The importance of overlay thickness was shown by disbonding occurring in a 5 mm thick overlay whereas none was observed in a 7 mm thick overlay exposed to identical autoclave conditions.

TECHNIQUES TO REDUCE OR PREVENT DISBONDING

Pressouyre et al (10) have suggested that if disbonding is to be avoided, preventive measures must be taken in the operation of pressure vessels. However, the operating options available for preventing disbonding are few, and probably impractical when emergencies arise. These options should draw on some technique to ensure that critical hydrogen levels do not occur during shutdown. This means either extensive degassing prior to shutdown or very slow cooling to permit the hydrogen to diffuse out of the pressure vessel walls.

The measures possible to prevent disbonding which can be applied at the manufacturing stage are numerous. It has been demonstrated in this work that a thicker overlay can reduce interfacial hydrogen build up. The chemistry of the base metal and the overlay strips can also be important considerations. Here the primary concern is to prevent carbide formation in the martensitic band and overlay grain boundaries. The carbon content of the 2 1/4 Cr-1 Mo should be reduced or a barrier placed between the base steel and the overlay, the carbon content at the interface being directly related to the base metal carbon content (2). Alternatively consideration may be given to

tying up the available carbon in strong (but widely dispersed) carbides such as NbC. Pressouyre et al (10) have shown 309 Nb to be better than 309 L in preventing disbonding and similar results have been reported by Sims and Bruck (11). It has also been suggested (4) that impurity elements segregate to the regions susceptible to disbonding and therefore the starting stainless steel strips and 2 1/4 Cr-1 Mo base metal should be low in certain trace elements such as Si, P and S.

Other important manufacturing considerations are the welding parameters during overlaying which can affect both interface chemistry and microstructures. Various workers (4,11) have shown that the large stainless steel grains with boundaries parallel to the interface are particularly susceptible to disbonding. The amount of δ-ferrite in the overlay should also be at the upper end of the range permissible for adequate overlay ductility (4). Also, it has been shown (4,10) that high speed welding with low dilution aids in preventing disbonding.

SUGGESTIONS FOR FUTURE WORK

The microstructural analysis of the interface band is incomplete. Identification of the particles in the martensite and overlay boundaries should be made with improved two-stage plastic replicas and/or ion beam thinned foils. Impurity element identification in grain boundaries should be attempted with Auger spectroscopy.

Stainless steel 308 L is also widely used as an overlay material for hydrocracking and hydrosulphurizing pressure vessels. Its disbonding susceptibility is controversial; some workers (9) report 308 L to have poor disbonding resistance while others (3) find it to be superior to other stainless steels.

The welding parameters used in applying the overlay are very important and although they have been extensively studied, further work would be useful. An analysis of the formation and morphology of intrusions or islands could be particularly informative because these morphological features appear to act as crack arrestors.

Carbon plays a major role in disbonding and future overlays should be produced using 2 1/4 Cr-1 Mo steel with carbon contents near 0.15% C.

A major problem in this work has been the difficulty of simulating the conditions in which disbonding occurs in practice. Fujii et al (12) have used hydrogen-charging from H_2S-saturated solutions to produce disbonding. However, Pressouyre et al (10) have shown that the profile developed by hydrogen charging does not duplicate that developed by cooling a pressure vessel.

ACKNOWLEDGEMENTS

The authors wish to express their indebtedness to the following PMRL personnel; R. Orr, Y. Lavoie, V. Chartrand, V. Moore and J. Newbury. Also the work done on the autoclave at ERL by Dr. F. Ng and co-workers is gratefully acknowledged.

REFERENCES

1. K. Ohnishi, R. Chiba, J. Watanabe, K. Naito and H. Okada, Japan Steel Works Report MR 80-17, Presented at Pressure Vessel Research Committee Meeting, New York; Sept. 1980.

2. R. Bondeau, G.M. Pressouyre, A Cheviet, J.A. Berthet and J.M. Duranseaud "Current solutions to hydrogen problems in steel"; 356-360, Washington; Nov. 1982, Pub. ASM.

3. H. Okada, K. Naito, J. Watanabe, K. Ohnishi and R. Chiba, ibid 331-339.

4. Anon, Kobe Steel Welding Technical Report 541; 1982, submitted to Welding Metallurgical Committee, JWS.

5. E. Zakaib (Petro-Canada Products, Ltd.), talk given to Montreal Section of NACE; April 12, 1983.

6. R.S. Chandel and R. Hoare, MRP/PMRL 80-80(TR); CANMET, Energy, Mines and Resources; 1980.

7. M.J. Godden, unpublished research; PMRL/CANMET, EMR; 1982.

8. W.E. Erwin and J.G. Kerr, Welding Research Council Bulletin 275; Feb. 1982.

9. K. Asami and T. Sakai, Trans. Iron and Steel Inst. of Japan, B266, vol. 21 (6); 1981.

10. G.M. Pressouyre, J.M. Chaillet and G. Valette, "Current solutions to hydrogen problems in steel"; 349-355, Washington; Nov. 1982, Pub ASM.

11. J.E. Sims and G.J. Bruck, "Performance of pressure vessels with clad and overlayed stainless steel linings"; Denver; June 1981, Pub. ASME, MPC-16.

12. T. Fujii, T. Hazama, H. Nakajima and R. Horita, "Current solutions to hydrogen problems in steels"; 369-378, Washington,; Nov. 1982, Pub. ASM.

13. T. Sakai, K. Asami, M. Katsumata, H. Takada and O. Tanaka, "Current solutions to hydrogen problems in steel"; 340-348, Washington; Nov. 1982, Pub. ASM.

14. T. Groeneveld and A.R. Elsea, "Permeation of hydrogen at elevated temperatures and pressures through stainless steel overlayed 2 1/4 Cr-1 Mo steel"; API Proceedings, vol. 56 (7-16); 1977.

14. K. Kinoshita, H. Itoh and A. Ebata, "Current solutions to hydrogen problems in steel"; 369-375, Washington; Nov. 1982, Pub. ASM.

Table 1. Material compositions used to produce overlays.

	C	Cr	Mo	Ni	Mn	Nb	Si	P	S	Ti	Cu
Base metal CSA 387 Grade 22 Class 2	0.11	2.34	0.95		0.48		0.22	0.011	0.022		
Stainless steel Strip 309	0.052	19.37	0.24	10.43	1.56	0.02	0.64	0.026	0.008	0.01	0.06
Stainless steel Strip 316 L	0.011	17.8	2.70	12.0	1.86		0.36	0.018	0.003		
Stainless steel Strip 347	0.018	20.3	0.07	10.1	1.66	0.61*	0.35	0.012	0.009	-	0.044

*Ta + Nb = 0.61

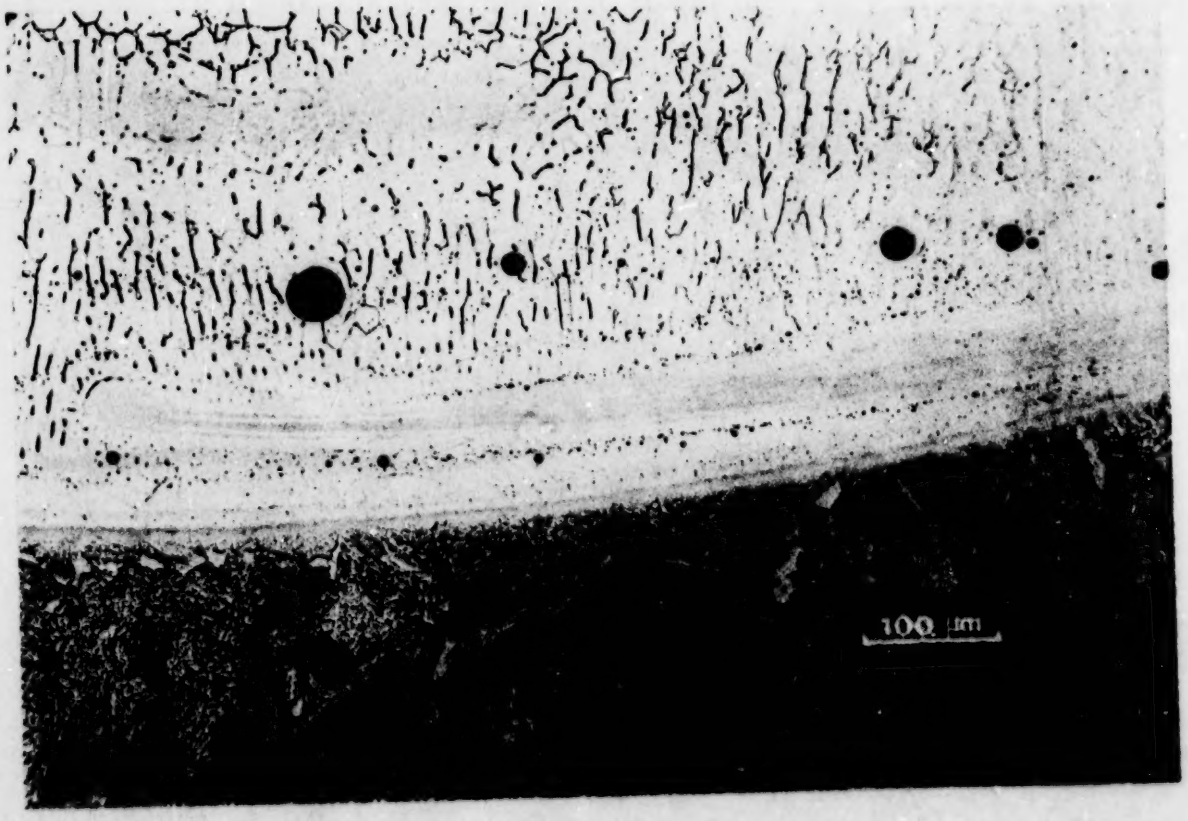

Fig. 1. As-welded 309/347 overlay, etched electrolytically at 5 V in 2% chormic acid for 45 s then etched in 2% nital for 30 s. Note islands and intrusion of 2 1/4 Cr-1 Mo steel in overlay and large number of spherical inclusions in overlay layer. (neg 9258)

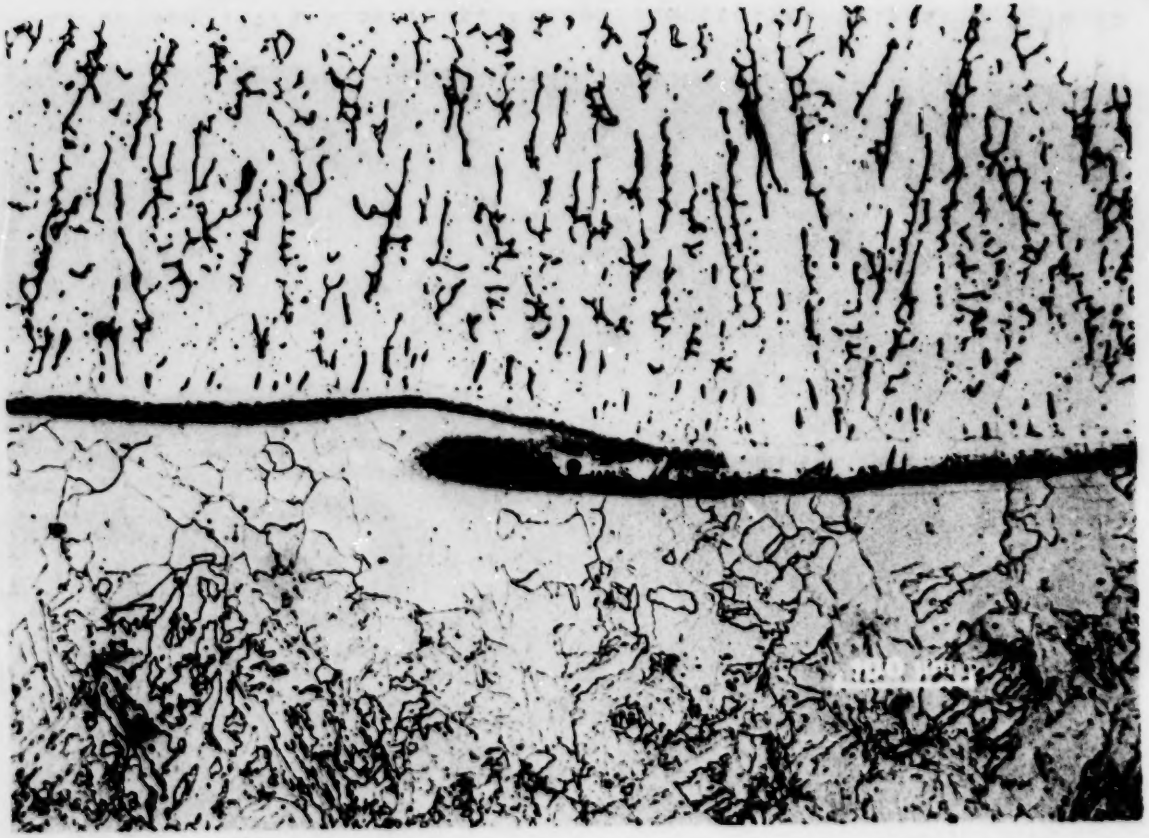

Fig. 2. 309/316 L overlay PWHT for 6 h at 690°C. Note tempered martensite band of variable width with an intrusion at the interface. (neg 9259)

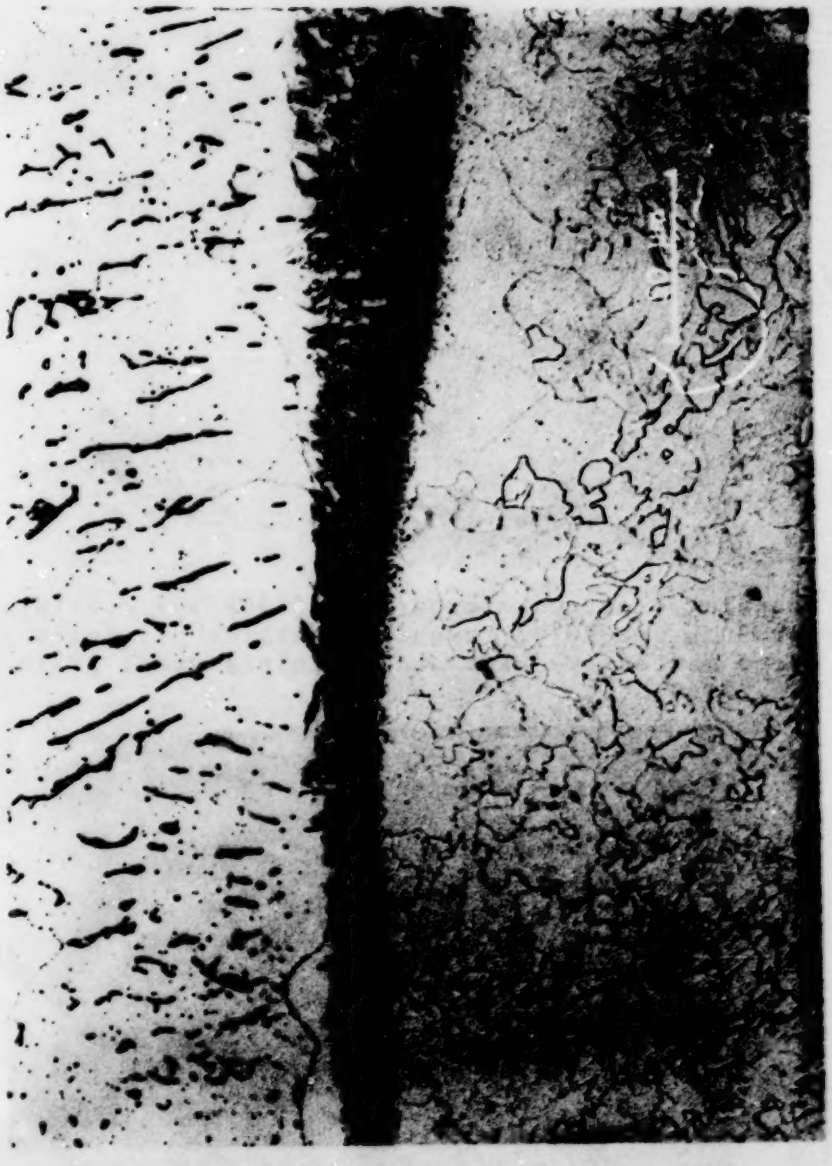

Fig. 3. 309/347 overlay PWHT for 30 h at 690°C. (neg 9257)

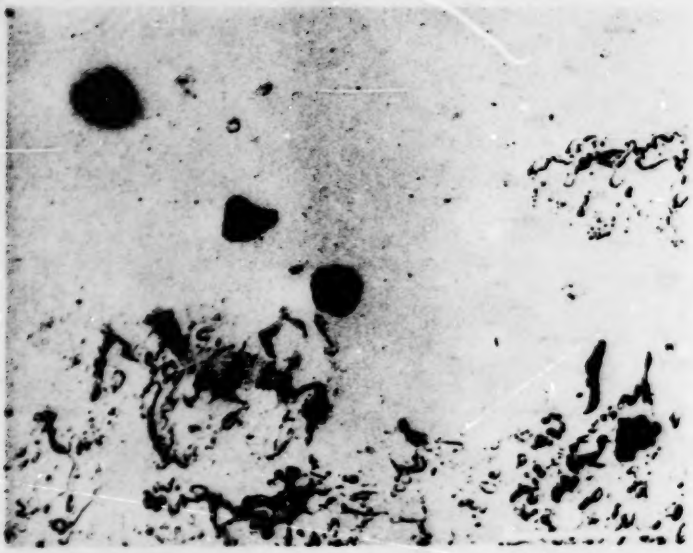

Fig. 4. Scanning electron micrograph of 309/347 overlay, PWHT for 30 h at 690°C, revealing carbide particles in tempered martensite band and stainless steel grain boundaries. (neg 9260)

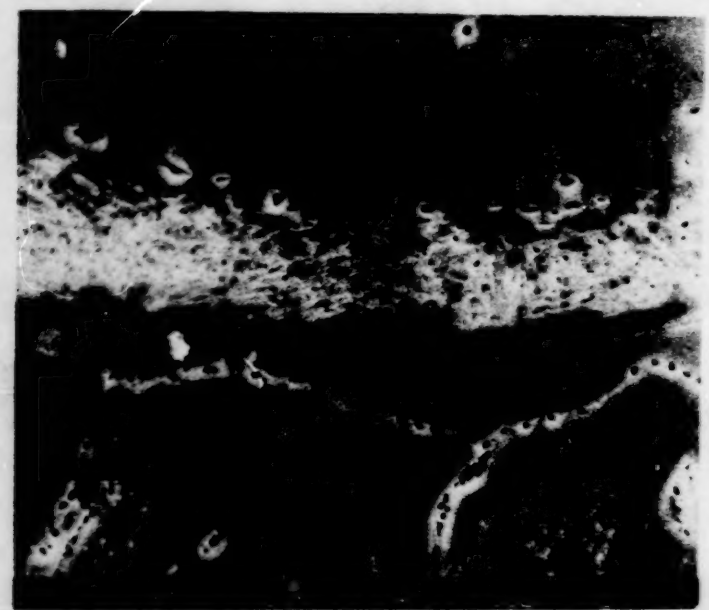

Fig. 5. Transmission electron micrograph showing particles extracted on a two-stage plastic replica. (neg 9261)

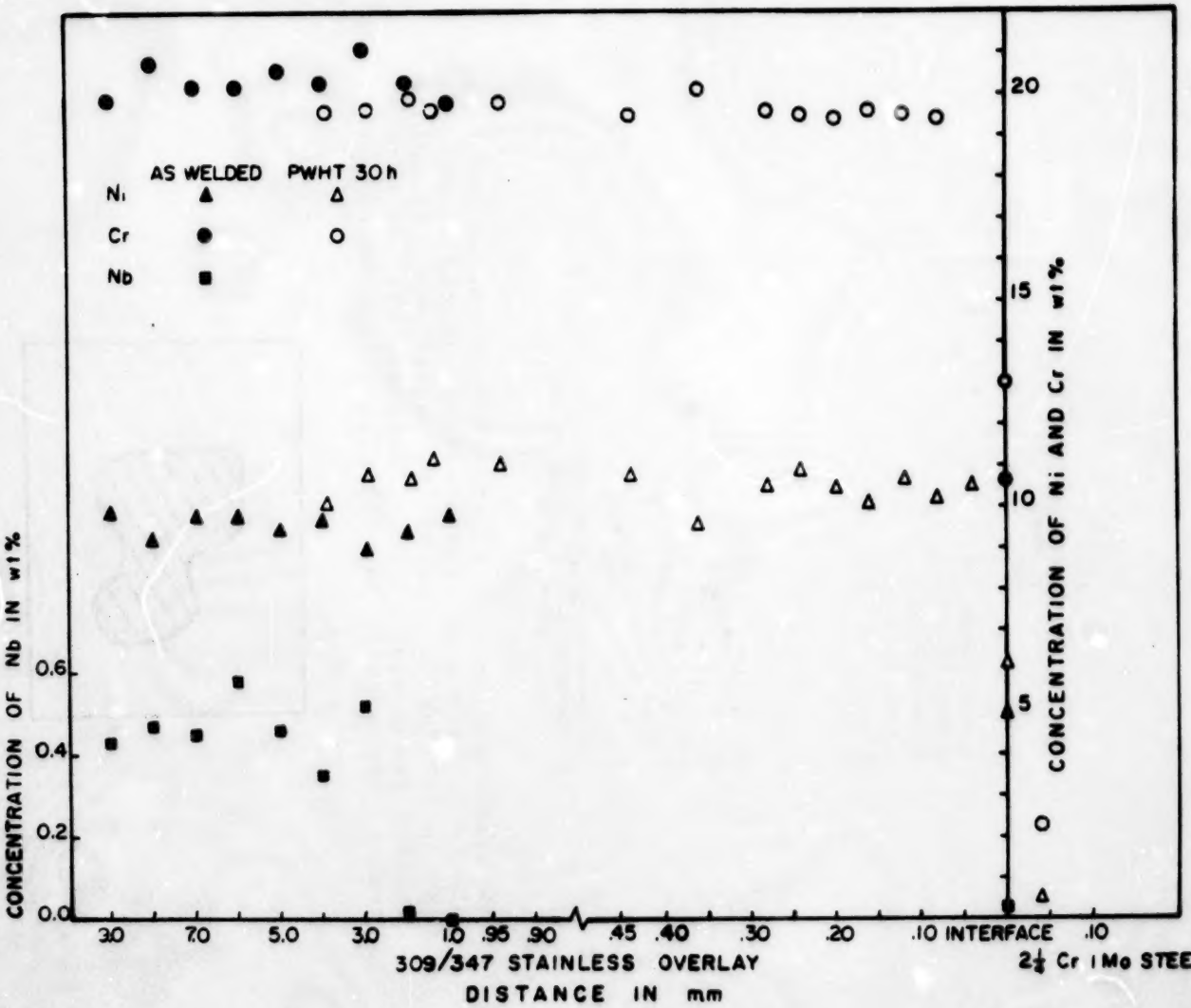

Fig. 6. Electron microprobe traces in the vicinity of the interface of a 309/347 overlay in the as-welded, and in the PWHT 5 h at 690°C, conditions. (neg 9266)

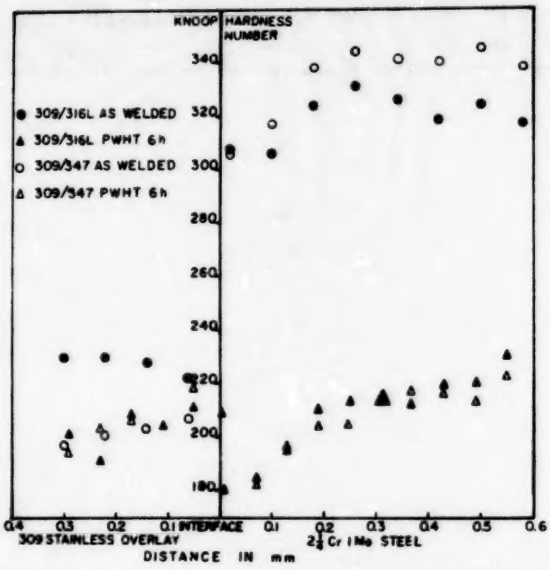

Fig. 7. Microhardness results in the vicinity of the interface of the interface of both overlays, in the as-welded, and in the PWHT 5 h at 690°C, conditions. As-welded results are a mean of five readings, PWHT results are a mean of three readings; 500 g load 1.25 mm obj. (neg 9263)

Fig. 8. Schematic diagram of disbonding, detected by ultrasonic inspection several days after autoclave exposure of a 309/347 overlay (approx. to full scale). (neg 9265)

Fig. 9. Disbonding crack in 309/347 overlay. Note crack ends at intrusion. (neg 9256)

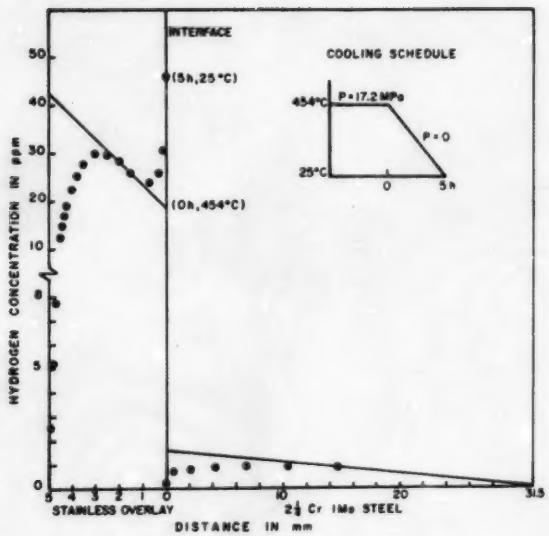

Fig. 10. Computer simulation of hydrogen profiles in 5 mm thick overlay sample at the completion of autoclave treatment and after cooling to ambient temperature Simulation is based on hydrogen uptake and loss through overlay surface only. (neg 9262)

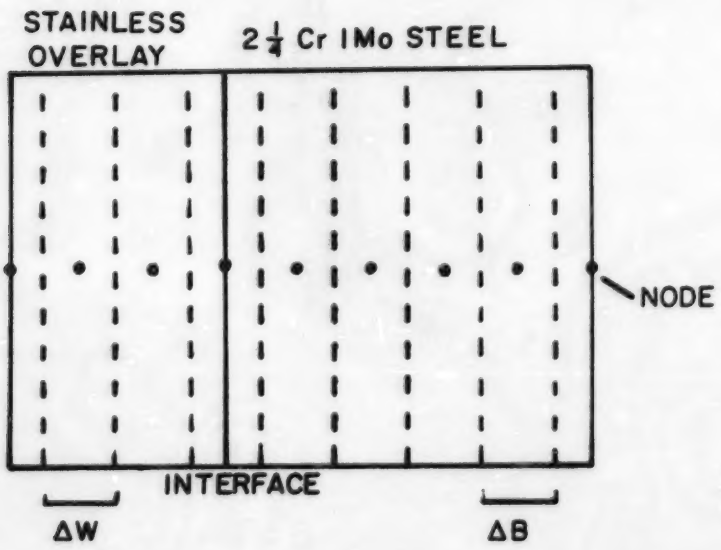

Fig. 11. Schematic diagram of stainless teeel weld overlay sectioned into elements to calculate the hydrogen distribution by the numerical explicit finite differences tehcnique. (neg 9264)

APPENDIX I

The FORTRAN IV computer program simulates hydrogen diffusion across pressure vessel material under steady state conditions and during the shut-down period. Hydrogen distributions were calculated by the numerical explicit finite differences technique. The weld overlay and base metal were sectioned into elements where each element was assigned a node (Fig. 11). The mathematical equations for calculating hydrogen concentrations were derived by performing a mass balance at each node using Ficks's first law of diffusion. The hydrogen concentration at the entry surface of the weld overlay was calculated by the equation:

$$Cw = Ks\ (P_{H_2})^{1/2} \qquad (1)$$

where P_{H_2} = hydrogen pressure of atmosphere (kg/cm^2)

K_s = solubility constant of weld overlay

Interfacial hydrogen concentrations in the weld overlay and base metal were calculated by the ratio of hydrogen concentrations for each material exposed directly to the hydrogen atmosphere:

$$Cw = \alpha C_B \qquad (2)$$

where $\alpha = K_s/K_B$

Note that the calculations are based on one dimensional diffusion of hydrogen. Further details on the calculation of hydrogen concentrations may be obtained from (13,14).

Diffusion coefficients and solubility constants were obtained from the literature (13,15). Solubility and diffusivity departures from normal behaviour at low temperatures were taken into consideration:

$K_B = 23.4 \exp(-3257/T)$

$= 1.8 \exp(-1789/T)$ ($\leq 300°C$)

$K_S = 7.6 \exp(-630/T)$

$D_B = 2.4 \times 10^{-3} \exp(-2132/T)$

$= 4.3 \times 10^{-4} \exp(-3358/T) \quad (\leq 150°C)$

$D_S = 7.11 \times 10^{-4} \exp(-4555/T)$

$= 6.0 \times 10^{-3} \exp(-5781/T) \quad (\leq 300°C)$

where K = solubility constant

D = diffusion coefficient (cm^2/sec)

T = temperature (°K)

S = stainless overlay

B = base metal.

COMPUTER PROGRAM

```
      REAL ITEMP, KS, KB, MB, MS
      INTEGER WNODE, BNODE
      DIMENSION CWELD (100), CBASE (100)
      WRITE (9,10)
10    FORMAT ('ENTER IN STEADY-STATE TEMP, DEGREES C')
      READ (9,*) ITEMP
      WRITE (9,15)
15    FORMAT ('ENTER IN THICKNESS OF WELD, CM')
      READ (9,*) WTHICK
      WRITE (9,20)
20    FORMAT ('ENTER IN HYDROGEN PRESSURE DURING STEADY-STATE, KG/CM2')
      READ (9,*) HPRESS
      WRITE (9,25)
25    FORMAT ('ENTER IN COOLING RATE, DEGREES C/HR')
      READ (9,*) COOLRT
      WRITE (9,30)
30    FORMAT ('ENTER IN THICKNESS OF BASE METAL, CM')
      READ (9,*) BTHICK
      WRITE (9,35)
35    FORMAT ('ENTER IN TIME INCREMENT, SEC')
      READ (9,*) DELTAT
      WRITE (9,40)
```

```
40    FORMAT ('ENTER IN SPACE INCREMENT OF WELD OVERLAY, CM')
      READ (9,*) DELTAW
      WRITE (9,45)
45    FORMAT ('ENTER IN SPACE INCREMENT OF BASE METAL, CM')
      READ (9,*) DELTAB
      WRITE (9,50)
50    FORMAT ('ENTER IN FINAL TIME, HOURS')
      READ (9,*) FTIME
      WRITE (9,55)
55    FORMAT ('ENTER IN HYDROGEN PRESSURE DURING SHUT-DOWN, KG/CM2')
      READ (9,*) PH2
      WRITE (9,60)
60    FORMAT ('ENTER IN NUMBER OF NODES IN BASE METAL')
      READ (9,*) BNODE
      PRINT *, 'OPERATING CONDITIONS'
      PRINT *, 'STEADY-STATE TEMP, C =', ITEMP
      PRINT *, 'STEADY-STATE PRESSURE, KG/CM2 =', HPRESS
      PRINT *, 'COOLING RATE, DEGREES C/HR =', COOLRT
      PRINT *, 'WELD THICKNESS, CM =', WTHICK
      PRINT *, 'BASE METAL THICKNESS, CM =', BTHICK
      PRINT *, ' '

C KS = SOLUBILITY CONSTANT OF WELD OVERLAY
C KB = SOLUBILITY CONSTANT OF BASE METAL
C DS = H2 DIFFUSION COEFFICIENT OF WELD OVERLAY
C DB = H2 DIFFUSION COEFFICIENT OF BASE METAL
C CW1, CWELD(1) = H2 CONC. AT ENTRY SURF. OF WELD OVERLAY
C CE2, CWELD (WNODE) = H2 CONC. IN OVERLAY AT INTERFACE
C CB3, CBASE(1) = H2 CONC. IN BASE METAL AT INTERFACE

C NUMBER OF NODES IN WELD
C
      WNODE = WTHICK/DELTAW + 1
C
C CALCULATION OF STEADY-STATE CONCENTRATIONS
C
```

```
      TIME = 0
      TEMP = COOLRT*TIME + ITEMP + 273.15
      KS = 7.6*EXP (-630/TEMP)
      KB = 23.4*EXP(-3257/TEMP)
      DS = 7.11E-4*EXP(-4555/TEMP)
      DB = 2.4E-3*EXP(-2132/TEMP)
      ALPHA = KS/KB
C
      CW1 = KS*HPRESS**0.5
      CB3 = DS*BTHICK*CW1/(DB*WTHICK + ALPHA*DS*BTHICK)
      CW2 = ALPHA*CB3
C
      PRINT *, 'STEADY-STATE CONCENTRATIONS (PPM) IN WELD OVERLAY'
      PRINT *, 'DIST. FROM SURF. TO INTERF.(CM)    H2 CONC (PPM)'
C
      X = 0
      DO 100, N = 1, WNODE
         CWELD(N) = (CW2 - CW1)/WTHICK*X + CW1
         WRITE (6,90) X, CWELD(N)

         X = X + DELTAW
100      CONTINUE
C
C     STEADY-STEADY CONCENTRATIONS IN BASE METAL
C
      PRINT*, 'STEADY-STATE CONCENTRATIONS (PPM) IN BASE METAL'
      PRINT*, 'DIST. FROM INTERF. (CM)    H2 CONC. (PPM)'
      B = 0
      DO 200, N = 1, BNODE
         CBASE(N) = -CB3*B/BTHICK + CB3
         WRITE (6,90) B, CBASE(N)
         B = N*(N + 1)*DELTAB/2
200      CONTINUE
C
350        IF(TIME.GE.FTIME) GO TO 600
C
```

```
      TIME = TIME + DELTAT/3600
      TEMP = COOLRT*TIME + ITEMP + 273.15
      IF(TEMP.GT.423.15.AND.TEMP.LE.573.15) GO TO 355
      IF(TEMP.GE.298.15.AND.TEMP.LE.423.15) GO TO 360
      GO TO 365
355   KB = 1.8*EXP(-1789/TEMP)
      KS = 7.6*EXP(-630/TEMP)
      DS = 6.0E-3*EXP(-5781/TEMP)
      DB = 2.4E-3*EXP(-2132/TEMP)
      GO TO 370
360   KB = 1.8*EXP(-1789/TEMP)
      KS = 7.6*EXP(-630/TEMP)
      DS = 6E-3*EXP(-5781/TEMP)
      DB = 4.3E-4*EXP(-3358/TEMP)
      GO TO 370
365   KS = 7.6*EXP(-630/TEMP)
      KB = 23.4*EXP(-3257/TEMP)
      DS = 7.11E-4*EXP(-4555/TEMP)
      DB = 2.4E-3*EXP(-2132/TEMP)
370   ALPHA = KS/KB
C
C     HYDROGEN CONCENTRATION IN WELD OVERLAY DURING SHUT-DOWN PERIOD
C
      MS = DS*DELTAT/DELTAW**2
      DO 300, N = 1, WNODE
        IF (N.EQ.1) GO TO 11
        IF (N.GE.2.AND.N.LT. WNODE) GO TO 22
        IF (N.EQ.WNODE) GO TO 33
11      CWELD(N) = KS*(PH2**0.5)
        GO TO 300
22      CWELD(N) = CWELD(N)*(1 - 2*MS) + MS*(CWELD(N + 1) + CWELD(N - 1))
        GO TO 300
33    CWELD(N) = (DS*CWELD(WNODE - 1)/DELTAW + DB*CBASE(2)/DELTAB)
      CWELD(N) = CWELD(N)/(DB)/(ALPHA*DELTAB) + DS/DELTAW)
300     CONTINUE
C
```

```
C     HYDROGEN CONCENTRATION IN BASE METAL DURING SHUT-DOWN PERIOD
C
        MB = DB*DELTAT/DELTAB**2
        DO 500, N = 1, BNODE
          IF (N.EQ.1) GO TO 44
          IF (N.NE.1) GO TO 66
44      CBASE(N) = CWELD(WNODE)/ALPHA
        GO TO 500
66        A = (N-1)*(N-0.5)
          C = N*(N-0.5)
        CBASE(N) = CBASE(N)*(1 - MB/A - MB/C) + (CBASE(N - 1)*MB/A)
        CBASE(N) = CBASE(N) + (CBASE(N + 1)*MB/C)
500   CONTINUE
      GO TO 350
600     PRINT *, ' '
        PRINT *, 'TIME, HRS =', TIME, C =', TEMP
        PRINT *, ('H2 CONC. (PPM) IN OVERLAY DURING SHUT-DOWN PERIOD')
        PRINT *, 'DIST. FROM SURF. TO INTERF. (CM)    H2 CONC (PPM)
      X = 0
        DO 700, N = 1, WNODE
      WRITE (6,90) X, CWELD(N)
      X = X + DELTAW
700   CONTINUE
      PRINT *, ('H2 CONC. (PPM) IN BASE METAL DURING SHUT-DOWN PERIOD')
      PRINT *, ' DIST. FROM INTERF. (CM)    H2 CONC (PPM)'
      B = 0
      DO 800, N = 1 BNODE
      WRITE (6,90) B, CBASE(N)
      B = N*(N + 1)*DELTAB/2
800   CONTINUE
90    FORMAT (13X, F10.7, 15X, F9.5)
      STOP
      END
```